# Organic Microporous Materials Made By Bicontinuous Microemulsion Polymerization

**J. H. Burban, Mengtao He, and E. L. Cussler**
Dept. of Chemical Engineering and Materials Science, University of Minnesota, Minneapolis, MN 55455

*Microporous solids made by polymerizing the organic phase of bicontinuous microemulsions stabilized with didodecyldimethylammonium bromide show surface areas as high as 70 $m^2/g$. Small-angle X-ray scattering measurements on microporous copolymers containing polymethylmethacrylate show that these areas result from structures larger than 250 Å that are generated during polymerization. These X-rays measurements also show that the 17-Å structures characteristics of the original microemulsion are retained during polymerization, but destroyed when the detergent is extracted and the solid is dried.*

## Introduction

This article and its companion (Burban et al., 1995) describe the synthesis of microporous materials made by polymerizing one continuous component of a bicontinuous microemulsion, and then removing the unpolymerized material. The hope is that the self-assembled, bicontinuous structure will be retained during the polymerization to produce a bicontinuous solid with unusually small pores. In a few cases, this hope is realized. In most cases, the structure partially collapses, apparently because removing the detergent from the polymer destroys much of the microemulsion structure.

This particular article is limited to the synthesis of organic polymers in microemulsions made with the surfactant didodecyldimethylammonium bromide. We chose this surfactant because it has been carefully studied and because it is known to yield an unusually large bicontinuous region (Chen et al., 1984, 1986; Chen, 1985). We chose both hydrophobic and oleophobic vinyl monomers whose polymerization is straightforward. Thus the work described here is a first step in making these microemulsion-based materials.

Our synthesis of these materials consists of four steps. The first step is the formation of a bicontinuous microemulsion containing a monomer. This monomer will concentrate in the hydrophilic domain if it is hydrophilic, or in the oleophilic domain if it is oleophilic. If the monomer is a liquid, it can partially replace either the oil or the water in the microemulsion. If the monomer is a solid, it must be dissolved in an appropriate solvent so that the resulting monomer solution can be used to make the microemulsion. For example, if the monomer is methyl methacrylate, the bicontinuous microemulsion will consist of surfactant, water, and methyl methacrylate. If the monomer is acrylamide, the bicontinuous microemulsion will consist of surfactant, oil, and a solution of acrylamide in water.

The second step of our synthesis is the polymerization of the monomer in the bicontinuous microemulsion. The conditions for the polymerization depend upon the monomer. For the monomers in this article, which polymerize by a free-radical mechanism, an initiator is included in the microemulsion. The polymerization is initiated thermally at 70°C, or by using ultraviolet light at room temperature.

The third step involves the removal of the nonpolymer components from the polymerized microemulsion. These include the surfactant, the unreacted monomer, the water, and any oil. This step is most readily accomplished by extraction, using a solvent that dissolves all the components except the polymer. The final step in the microporous material synthesis is the removal of the extraction solvent by vacuum or supercritical drying.

In the following sections, we first detail the synthesis of these materials, and then report their experimental characterization. This characterization, which emphasizes small-angle X-ray scattering, shows the extent to which the microemulsion structure is retained. Finally, we explore the mechanisms that are apparently involved, and suggest how more porous materials could be obtained.

Correspondence concerning this article should be addressed to E. L. Cussler.

## Experimental

In this section we detail the procedures followed when making microporous materials, starting with hydrophobic vinyl monomers. Similar procedures for hydrophilic vinyl monomers are described elsewhere (Burban, 1993). For the hydrophobic cases, the bicontinuous microemulsions consist of surfactant, water, and hydrophobic monomer. The hydrophobic monomers that we investigated are methyl methacrylate, butyl methacrylate, and styrene, each polymerized by a free-radical mechanism.

The polymerization of a bicontinuous microemulsion containing methyl methacrylate is typical. The reagent-grade materials required in this synthesis are the monomer methylmethacrylate (Aldrich), the cross-linker ethylene glycol dimethacrylate (Aldrich), the surfactant didodecyldimethylammonium bromide (Eastman), the initiator azobisisobutyronitrile (Aldrich), absolute ethanol (Eastman), and cyclohexane (Fischer). Azobisisobutyronitrile is recrystallized from methanol. Water is distilled twice, deionized once, and stripped of dissolved oxygen by degassing with nitrogen. The methyl methacrylate and the ethylene glycol dimethacrylate are washed three times with an equal volume of 10 wt. % KOH to extract the hydroquinone inhibitors. The monomers are then rinsed three times with equal volumes of distilled deionized water to remove any traces of KOH. Dry nitrogen is bubbled through the monomers to remove any dissolved oxygen.

In one typical group of experiments, the bicontinuous microemulsion is formed by mixing the ingredients in the following proportions: 66.4 wt. % didodecyldimethylammonium bromide, 7.1 wt. % water, 26.2 wt. % oil, and 0.3 wt. % azobisisobutyronitrile. The oil component is a mixture of 40% by weight methyl methacrylate and 60% by weight ethylene glycol dimethacrylate. The initiator, azobisisobutyronitrile, is dissolved into the monomer mixture before the components are mixed. The mixture forms a clear microemulsion with relatively gentle stirring. To demonstrate its bicontinuous nature, we measure the electrical conductivity of a series of similar microemulsions ranging from 4 to 11 wt. % water. Using a cell of constant 0.088 $cm^{-1}$, we find that the conductivity is around 5 mmho, somewhat below that typical of a salt solution, but well above that of oils (Burban, 1993).

The clear microemulsion is polymerized in a capped glass vial at 7° C for 1 h. During the polymerization, the initially clear microemulsion changes into a white solid, implying a phase change. No macroscopic phase separation occurs, and the volume of white solid formed is within 3% of the volume of the initially clear bicontinuous microemulsion. The white solid is extracted with absolute ethanol. The ethanol is replaced several times until no detectable surfactant remains. The solid shrinks with vacuum-drying. Freeze-drying with cyclohexane followed by vacuum-drying gives less shrinkage, typically less than 5 volume percent.

We measure the changes in the microemulsion structure during polymerization by means of small-angle X-ray scattering. These experiments are performed on a modified Kratky camera (Anton Paar KG, Graz, Austria) equipped with an extended flight tube and a movable beam stop (Kaler, 1982). The X-ray generator has a rotating anode (model RU-200B, Rigaku Corp., Japan), operating at 10 kW with a copper target. The $K_\alpha$ wavelength of 1.54 Å is selected by means of Nickle filters. The energy window on a Braun model OED-100-M 10-cm linear position-sensitive detector (Innovative Technology, Inc., Newburyport, MA) is set to accept only the scattering photons with energy close to 1.54 Å. The Kratky linear collimation produces a $3 \times 0.13$ $mm^2$ X-ray area (elongated pinhole) on the sample sealed in a 1.5-mm-ID glass capillary (Charles Supper Co., Natick, MA). The sample-to-detector distance was set at 68.2 cm. The detectable wave vector $q$ range is from 0.02 $Å^{-1}$ to 0.3 $Å^{-1}$, where $q$ is $(4\pi/\lambda) \sin(\theta/2)$ and $\theta$ is the scattering angle. The transmission coefficients are determined for each sample using the Siemens D-500 Diffractometer. The incident and transmitted intensities of samples placed in 1.0-mm capillaries are used to compute the transmission coefficient of the samples (Bohlen, 1990). The scattering data, accumulated over 30 to 240 min, are corrected for background by subtracting the scattering intensity of the background and the empty capillary. They are corrected for exposure time by multiplying the scattering intensity by $[10^4(s)/(\text{exposure time (s)})]$.

We measure the surface area of our microporous solids using both the single-point and multipoint methods with nitrogen as the adsorbate. The single-point surface area measurements are done on a Leeds and Northrup Model 4200 Automatic Surface Area Analyzer. Based on the linearized BET theory, the analyzer calculates the surface area from measurements of the volume of $N_2$ gas adsorbed and desorbed by the sample. To measure adsorption and desorption values, the analyzer utilizes the continuous-flow method. In this method, a mixture of 30% $N_2$ and 70% He is passed through a glass cell containing the sample. The cell is cooled in a liquid $N_2$ bath at $-196°$ C, which causes the $N_2$ gas in the feed mixture to be adsorbed by the sample. When no more $N_2$ gas adsorbs, the liquid $N_2$ bath is automatically removed and desorption occurs as the sample warms to room temperature. Desorbed $N_2$ from the sample passes through a thermal-conductivity detector, which produces an electrical signal proportional to the volume of $N_2$ desorbed. The signal is measured and summed by a digital integrator. Because the integrator is calibrated by injecting a precise volume of $N_2$, its output is read directly in units of surface area.

The multipoint surface area measurements are performed on Porous Materials Automated BET Sorptometer controlled by an IBM PC. The basis of sorptometer operation is as follows. A quantity of pure nitrogen gas is admitted into a known system volume. A calibrated pressure transducer is used to measure the system pressure and, based on the ideal gas law, the total number of moles of nitrogen gas. A sample valve is then opened, allowing the gas to expand into the sample chamber, which is maintained at $-196°$ C. The sample chamber is initially at very low vacuum and the surface of the sample is assumed to be free of any adsorbed gases. The pressure decreases due to expansion of the gas into a larger volume and due to the adsorption of nitrogen on the surface of the sample. Therefore, the sorptometer calculates the amount of nitrogen adsorbed onto the surface of the sample from measurements of the pressure in the system before and after adsorption. The sorptometer repeats this procedure at different pressures, increasing the pressure relative to the critical pressure up to approximately 0.30. The computer then fits the data to the BET equation to determine the surface

area. Good correlations are usually obtained with five or six data points.

The calculation of the specific surface area also requires knowing the skeletal density, that is, the density of the material making up the framework of the porous solid. This density equals the reciprocal of the difference between the reciprocal of the bulk density and the specific pore volume. The bulk density is just the mass of material divided by its total volume, including both solid and pores. The specific pore volume is determined by helium pycnometry. Because helium is a small, nonadsorbing species, it penetrates all sizes of pores, and so gives a measure of total pore volume in a sample of known mass.

We determine the pore-size distributions of our porous solids by combining nitrogen sorption with mercury porosimetry measurements. The principle of operation of the nitrogen desorption measurements is the same as presented earlier, except that the relative pressure range is extended to near unity. The pore-size calculations are based on the Kelvin equation, modified to include the thickness of the nitrogen layer in pores that are not yet filled. These experiments are used to determine the size distribution of pore radii ranging from 10 to about 250 Å. The pores greater than 250 Å in radius are measured using a Porous Materials Automated Porosimeter model number PMI 30K-A-1, controlled by an IBM PC. This porosimeter is operated in pressure mode, by controlling the applied pressure and measuring the intrusion volume. High pressures are generated with a piston, using isopropyl alcohol as the hydraulic fluid. The volume of mercury forced into a sample is measured with a penetrometer. The intrusion data are analyzed with the Washburn equation to obtain a cumulative pore volume determination, which is differentiated to give the pore-size distribution (Gregg and Sing, 1982). We recognize that the pressures ( $< 150$ atm) used here may deform the microporous matrix; we take solace in the fact that these measurements are not important to our conclusions, but are only made for completeness.

## Results

The properties of the organic microporous materials made by the procedure just discussed are summarized in Table 1. The first column in this table gives the monomer and the cross-linker of the microemulsion from which the material is made. The second column gives more details about the clear microemulsion's composition. The third column gives the material's appearance after polymerization but before drying. While the original microemulsions were clear, those based on oleophilic monomers like styrene became opaque during the polymerization. While we do not know the percent conversion where this opacity appears, we believe that this represents a microscopic phase separation due to the limited solubility of the polymer. In contrast, the materials based on hydrophilic monomers like acrylic acid remained clear, implying that no microscopic phase separation occurs in these cases. The remaining columns in Table 1 describe the dried solids. Column four gives the dried polymer density; the smaller values reflect our effort to make solids with an unusually high void fraction. The last column in the table gives the surface area per volume, measured most often by nitrogen adsorption.

To explore the origins of the results in Table 1, we focus on copolymers of methyl methacrylate and ethylene glycol dimethacrylate at the composition given in the preceding experimental section. We chose this system because it polymerized relatively easily to give reproducible results. We first combine nitrogen sorption and mercury porosimetry to determine the pore-size distribution of the dried material. The results, given in Figure 1, show a wide distribution of pore radii ranging from 10 to 1,000 Å. The largest peak occurs at an

**Table 1. Organic Microporous Solids Made from Polymerization of Bicontinuous Microemulsions***

| | Composition (wt. %) | Polymer Appearance before Drying | Polymer Density ($g/cm^3$) | Surface Area Vol., $m^2/cm^2$ |
|---|---|---|---|---|
| *Hydrophobic Monomer*** | | | | |
| Methylmethacrylate + Ethylene glycol Dimethacrylate (EGDM) | DDAB 42.7 to 66.2<br>Water 5 to 33.2<br>Oil 9.1 to 47.7 | Opaque | 0.07 to 0.46 | 3 to 70 |
| Styrene + divinyl benzene | DDAB 60.6<br>Water 23.1<br>Oil 16.3 | Opaque | 0.05 to 0.09 | 2 to 21 |
| Butyl methacrylate + EGDM | DDAB 59.8<br>Water 23.8<br>Oil 16.3 | Opaque | 0.25 | 22 |
| *Hydrophilic Monomer*†* | | | | |
| Acrylic acid + EGDM | DDAB 52.2<br>Decane 23.7<br>Monomers 24.1 | Transparent | 0.25 | 4 |
| Methacrylic acid + EGDM | DDAB 52.3<br>Decane 23.6<br>Monomers 24.1 | Transparent | 0.25 | 23 |

*DDAB is didodecyldimethylammonium bromide.
**These microemulsions consist of DDAB, water, and the hydrophobic monomer.
†These microemulsions consist of DDAB, decane, and the hydrophilic monomer.

average pore radius of about 250 Å. The results in Figure 1 are uncertain in two ways. First, we are not sure that the data below 20 Å are reliable (Gregg and Sing, 1982). Nitrogen adsorption depends on the assumptions used in the derivation of the Kelvin equation. The key assumption is that the properties of the condensed phase are the same as those of the liquid. This assumption breaks down when the pores are only a few molecular diameters wide. Second, a peak at 800 Å is seen in the mercury porosimetry data. While we are not sure of the origin of this peak, it may result from the phase separation that apparently occurs during extraction and drying.

These measurements show that the final structure of the porous solid is very different than that expected from the original microemulsion. Had the synthesis occurred without any changes, we would expect a large peak in the pore-size distribution at roughly two or three times the size of a detergent molecule. We expect that this pore size would correspond to the radius of the water conduits plus the length of the extended surfactant tails, and so be 15–30 Å. These sizes are much smaller than the radii calculated from the principal peaks in Figure 1.

Thus the data in Figure 1 imply that much of the microemulsion structure is not captured in the final microporous material. Instead, the material must undergo substantial rearrangement at one or more steps in the synthesis. Because of this rearrangement, the surface area of the resulting material is significantly less than expected. The specific surface area of the sample described earlier is 66 $m^2/g$. Based on the interfacial area of the surfactant molecules and the microemulsion composition, we might have expected a value of about 750 $m^2/g$. Thus we are losing over 90% of the potential specific surface area.

To see why the surface area is lost, we turn to small-angle X-ray scattering of the microemulsions during polymerization. The composition used for these experiments is slightly different than that in Figure 1: 45.5 wt. % didodecyldimethylammonium bromide, 45.5 wt. % monomer mixture, and 9.0 wt. % water. The monomer mixture consists of 20 wt. % methyl methacrylate and 80 wt. % ethylene glycol dimethacrylate. The initiator azobisisobutyronitrile is dissolved in the monomer mixture at 1 wt. % based on the total monomer.

The scattering profile for the microemulsion before polymerization, shown in Figure 2, shows a single peak, typical for bicontinuous microemulsions (Bohlen, 1990). This peak, which occurs at a scattering vector of 0.186 $Å^{-1}$, suggests that the average characteristic size is 17 Å (Brumberger, 1967). This size most probably corresponds to the interconnected, detergent-lined water conduits within the oil continuum.

More information about these small pores could conceivably be determined from a Porod analysis (Glater and Krathy, 1982). Such an analysis requires measurements at large scattering vector $q$. When we tried to make these measurements, we found considerable noise, requiring very long measurements (Burban, 1993). Accordingly, we abandoned this form of analysis and used only peak position to determine the smallest characteristic sizes.

We also measure the scattering from a bulk sample of polymethyl-methacrylate-coethylene glycol dimethacrylate, as shown in Figure 3. When this sample is made, the monomers are in the same ratio as those used in the microemulsion,

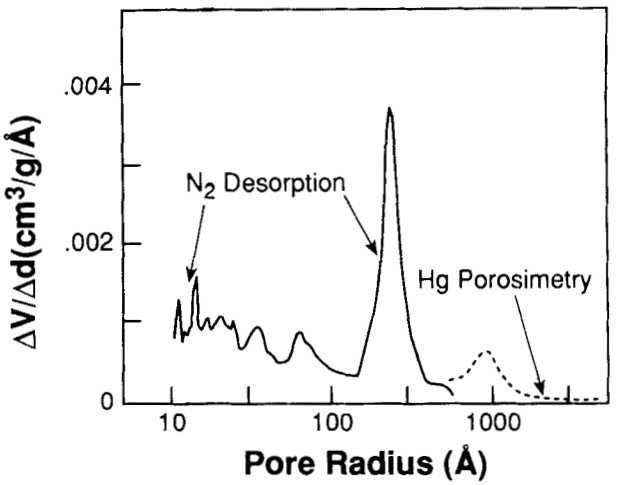


**Figure 1. Pore-size distribution of polymethylmethacrylate-coethylene glycol dimethacrylate.**

The solid shows a broad pore-size distribution with a sharp maximum at 250 Å.

though no detergent and water are present. The scattering profile of this polymer is completely different from the microemulsion scattering profile. A peak in scattering intensity is not observed, nor is it expected. The scattering intensity is much larger, at least at small scattering vectors. This intensity decreases rapidly with increases in scattering vector. The intense scattering at low scattering vector is attributed to the cross-linked polymer. An apparent size can be determined from the data in Figure 3 using the Guinier analysis, as illustrated by the data in the inset (Guinier and Fournet, 1955). The meaning of this size is unclear, probably because we are outside of the range where the Guinier analysis is exact.

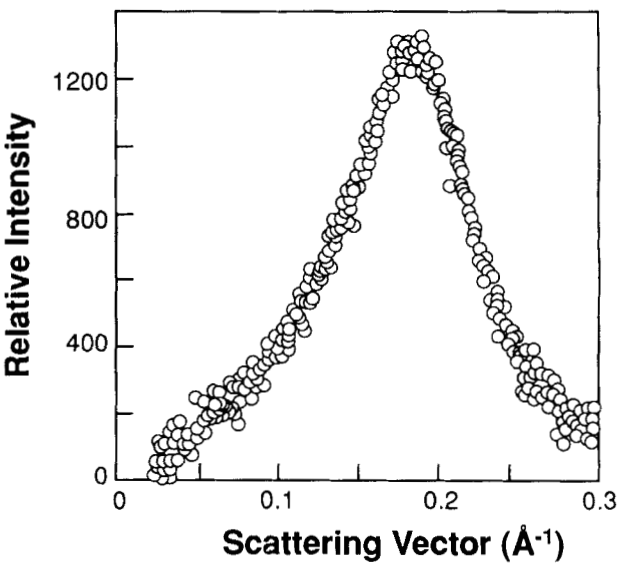


**Figure 2. Small-angle X-ray scattering of a microemulsion before polymerization.**

The clear microemulsion has an oil phase of methylmethacrylate and ethylene glycol dimethacrylate, though at a somewhat different concentration than in Figure 1. The peak corresponds to a characteristic size of 17 Å.

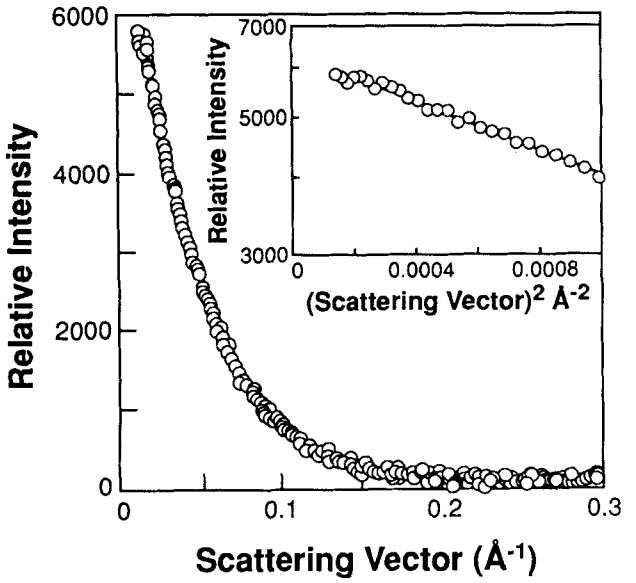


**Figure 3. Small X-ray scattering of a copolymer of methylmethacrylate and ethylene glycol dimethacrylate.**

Because this system contains no detergent, no microemulsion peak is observed.

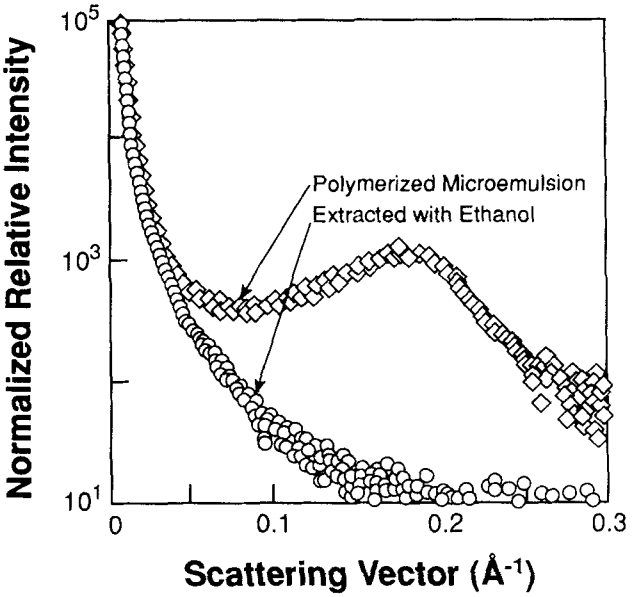


**Figure 5. Small-angle X-ray scattering before and after detergent extraction.**

Extraction apparently destroys the microemulsion structure, though not the larger, polymerization-engendered structure.

The scattering profiles for this bicontinuous microemulsion during polymerization are shown as a function of time in Figure 4. Note that this plot is semilogarithmic, while those in Figures 2 and 3 are Cartesian. The profiles in Figure 4 combine the features of the initial microemulsion and of the bulk polymer. Specifically, the peak associated with the microemulsion remains unchanged during the polymerization. A sharp increase in scattering at low scattering vector also develops as the polymerization proceeds.

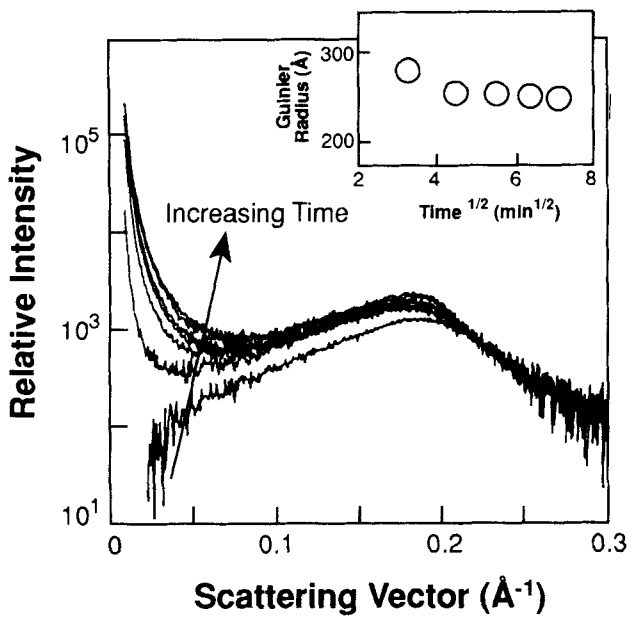


**Figure 4. Small-angle X-ray scattering of a microemulsion during polymerization.**

The peak at a scattering vector of 0.19 Å, which is characteristic of the microemulsion, is retained, while a peak characteristic of the polymer develops at low scattering vector. The size found from a Guinier analysis at low scattering vector is constant over time (inset).

These results imply that the cross-linked polymer has a structure like kernels of popcorn that are stuck together. The holes within each kernel, which have a size around 17 Å, are due to the microemulsion and do not change much during the polymerization. The kernels themselves are much larger, but their size is uncertain. When we apply a Guinier analysis to these data, we find a time-independent size of 250 Å, temptingly close to the 250-Å peak in Figure 1. However, we are outside the range where the Guinier analysis is exact, so this assignment is unproved. We know only that we have a new larger structure, which could be the peak in Figure 1 at 250 Å or that at 800 Å. This result echoes those of Carver et al. (1989) and Walsh et al. (1994), both of whom found new larger structures that appeared during polymerization.

Thus the polymerization retains the small-size characteristic of the microemulsion structure, and it generates a new, larger structure that does not change with time. At this point, we believe that we still have the very large surface area that we seek in these materials. To see where we lose 90% of this area, we must look at the subsequent steps of our procedure.

We next measure the small-angle X-ray scattering of samples before and after extraction with ethanol. This extraction, which removes the detergent, destroys the 17-Å peak associated with the microemulsion, as shown in Figure 5. To be sure, this change might conceivably be due to the removal of the bromide counterion, which causes a sharp contrast in the scattering. We believe the simpler explanation, that the extraction destroys most of the microemulsion structure and hence is the reason we lose so much potential surface area per volume.

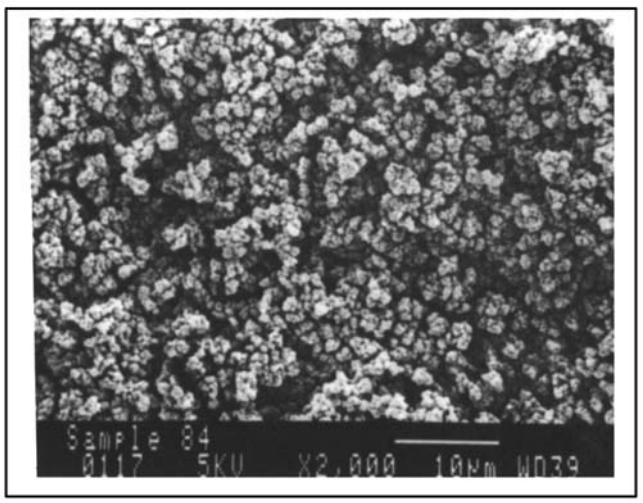


**Figure 6. Typical microporous material.**

This material is made by the polymerization of a bicontinuous styrene microemulsion.

We tried to explore this larger size observed with X-ray scattering by means of scanning electron microscopy, but were frustrated by the low resolution with these organic materials. A typical micrograph is shown in Figure 6. We can see abundant submicron structure, which may correspond to the 800-Å peak found by mercury porosimetry, but we cannot see much that is smaller. In addition, we measure the surface area per pore volume in a selection of dried microporous solids by varying the average functionality and the composition of the microemulsion. In four sets of experiments, we hold the composition of the bicontinuous microemulsion constant while varying the average functionality of the monomer mixture. For a fifth set of experiments, we hold the average functionality of the monomer mixture constant and vary the composition of the bicontinuous microemulsion across the phase diagram. A sixth set of experiments varies both the average functionality and the compositions in an unsystematic way. In all cases, the polymerized materials were extracted and dried in an identical fashion (Burban, 1993).

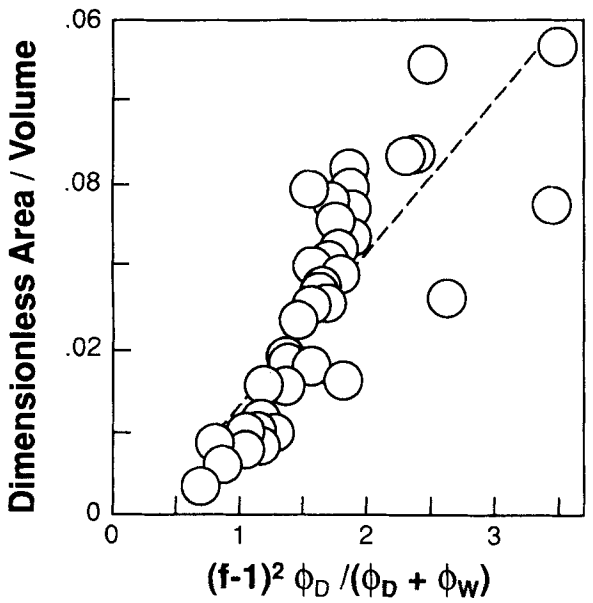


**Figure 7. Surface areas of dried microemulsion-based copolymers.**

The areas are increased by polyfunctional monomers and by more detergent.

The areas obtained for these samples are shown in Figure 7. In this figure, the ordinate is the measured area per pore volume (SA/PV), made dimensionless by multiplying by the sum of the molecular volumes of water (30 Å$^3$) and surfactant (700 Å$^3$) and by dividing by the surface area per detergent molecule (60 Å$^2$). The abscissa in Figure 7 is an empirical combination of the average functionality $f$ of the monomer mixture and of the volume fractions of water $\phi_W$ and of detergent $\phi_D$. Since the surface areas are reproducible within perhaps 30%, the correlation, with an $R^2$ of 0.82, seems reasonable. We will rationalize this empirical combination in the discussion that follows.

Before beginning this discussion, we should stress that the areas in Figure 7 are those found after the four steps of emulsion formation, polymerization, extraction, and drying. The results in Figure 5 imply that much of the local microemulsion structure is destroyed by the extraction step. Presumably, more might be destroyed by the drying step. Thus any discussion of the results in Figure 7 must include consideration of this altered structure.

## Discussion

The research described in this article tries to make microporous solids using bicontinuous microemulsions as templates. In other words, we want to polymerize the monomer present in one phase of a bicontinuous microemulsion to make a solid with an unusually high surface area per volume. If we are successful, we will have made a high surface area solid that can be used as an adsorbent or as a catalyst support. The high surface area can potentially be greater than that in other solids, including activated carbons.

Our results, given earlier, show mixed success. We can make microemulsions with a vinyl monomer in either the oil phase or the water phase. We can successfully polymerize this monomer. This polymerization can sometimes lead to phase separation, signaled by the initially clear microemulsion becoming opaque. Interestingly, the polymerization does not seem to destroy the microemulsion structure, even when it leads to phase separation. Our evidence of this retained structure is that the 17-Å size associated with the microemulsion remains unaltered by polymerizing methylmethacrylate-coethylene glycol dimethacrylate, a system that does show phase separation. The polymerization of the microemulsion does produce a new, larger size. The new size appears to be retained when this polymer is dried.

In contrast, the detailed microemulsion structure, which is retained in the polymerization, is destroyed by the extraction. It does not reappear in the drying. What structure is retained still gives significant surface areas of around 50 m$^2$/g (cf. Table 1), consistent with the larger-size characteristic of the polymerization, but not with the size characteristic of the microemulsion (about 17 Å). This implies that two polymer

chains easily cuddle together once any detergent lamellars are extracted. Still, the results in Figure 7 show that more area is retained for systems with more cross-linking and with more detergent.

Thus the preceding results show that polymerizing bicontinuous microemulsions can give highly microporous solids, but that much of the microstructure is lost when the surfactant is removed. Still, the results are frustratingly incomplete, for they raise at least four major questions:

1. What is the source of the new size that appears during polymerization?
2. What is responsible for the surface area variation with microemulsion concentration?
3. How do our results compare with other microemulsion polymerizations?
4. How can we avoid losing the detailed microemulsion structure during extraction and drying?

We will explore the answers to these questions next.

First, we suspect that the source of the new structure formed during polymerization results from precipitation. If this picture is correct, polymerization would take place in small monomer regions that incorporate microemulsion structure. The polymerization would proceed rapidly until the polymer precipitates by spinodal decomposition induced by the higher free energy of the chains. This mechanism, which seems a rough parallel to the "polymerization in water" theories of emulsion polymerization (Poehlein, 1986), is also consistent with the linear variation of surface area with surfactant. However, it seems inconsistent with systems like microporous polyacrylic acid, which show no evidence of phase separation during polymerization.

We can use similar arguments to partially answer our second question, about why the surface area varies with microemulsion concentration. We expect a vinyl polymerization to center on the reaction between a monomer and an active chain. Such a reaction should be second order, depending on the square of the average functionality in the system. This expectation is consistent with the variation of surface area with $(f-1)^2$ shown in Figure 7. Similarly, we expect that the pore volume would vary with the total volume fraction of detergent $\phi_D$ and of nonsolvent $\phi_W$, and that the surface area would be proportional to the concentration of the surface-forming detergent. These expectations are also supported by Figure 7, where the surface area per pore volume varies with $\phi_D/(\phi_D + \phi_W)$. This correlation may be accidental, because most of the detergent is presumably involved in the smaller microemulsion structure, and that smaller structure is destroyed by extraction before the surface area is measured.

To answer our third question, we must compare our results with others in the literature. Most microemulsion polymerizations ape conventional emulsion polymerization by putting the monomer in small dispersed droplets (Candau, 1992). They are not bicontinuous; they have the monomer in the dispersed phase. On polymerization, they routinely produce latex particles an order of magnitude larger than that expected from the size of the original droplets (Candau et al., 1984; Johnson and Gulari, 1984; Guo et al., 1989; Brouwer, 1989; Perez-Luna et al., 1990; Candau, 1989; Gan et al., 1991). The mechanism for forming these larger particles, sometimes described as agglomeration or coagulation, may be related to the same mechanism responsible for the larger sizes observed here (Kuo et al., 1987; Larpent and Tadros, 1991; Guo et al., 1992 a,b).

Other studies of microemulsion polymerization have used bicontinuous networks rather than dispersed droplets (Qutubuddin et al., 1989; Friberg et al., 1989, 1992a,b; Walsh et al., 1994). Some of these studies have attempted polymerization in both phases, producing interpenetrating polymer networks (Qutubuddin et al., 1989). These materials, often characterized rheologically, show curious combinations of the properties of the pure polymers (Friberg et al., 1992). Cheung and his coworkers (Raj et al., 1991, 1995), in a series of strong articles, also measured X-ray scattering of the final microemulsions. Others work involving polymerization of inorganic monomers will be described in more detail in the companion article (Burban et al., 1995).

Finally, we want to repeat our fourth question, about how we might retain the smaller microemulsion structure destroyed during extraction and drying. While one chance of retaining this structure is to use more highly cross-linked monomers, we have tried this in this article without great success. Other, more promising alternatives might be to use detergents containing vinyl groups or to initiate polymerization at detergent concentrations containing more rigid structures than those typical of bicontinuous microemulsions. Another alternative might be radiation curing before extraction. So far, we have experienced considerable frustration: we seem to capture the microemulsion structure with any monomer, but we lose most of it on detergent extraction. We will keep trying.

## Acknowledgments

The work was supported by the Advanced Research Projects Administration (grant 92-05112) and by the National Science Foundation (grant CTS91-23837). The authors are indebted to Prof. Mark D. Foster, University of Akron, for his careful review of this article.

## Literature Cited

Bohlen, D. S., "Small X-Ray Scattering Exploration of Nonionic Microemulsion Structure," PhD Thesis, Univ. of Minnesota, Minneapolis (1990).

Brouwer, W. M., "The Preparation of Small Polystyrene Latex Particles," *J. Appl. Poly. Sci.*, **38**, 1335 (1989).

Brumberger, H., "Small Angle X-Ray Scattering," *Proc. Conf. Syracuse University*, H. Brumberger, ed., Gordon & Breach, New York (1967).

Burban, J. H., "Microporous Materials Based on Bicontinuous Microemulsion Polymerization," PhD Thesis, Univ. of Minnesota, Minneapolis (1993).

Burban, J. H., M. He, and E. L. Cussler, "Silica Gels Made by Bicontinuous Microemulsion Polymerization," *AIChE J.*, **41**, 159 (1995).

Cabane, B., in *Surfactant Solutions: New Methods of Investigation*, R. Zana, ed., Marcel Dekker, New York, p. 58 (1987).

Candau, F., "Polymerization of Water-Soluble Monomers in Microemulsions: Potential Applications," *Polymer Association Structures*, M. A. El-Nokaly, ed., Washington, DC, p. 47 (1989).

Candau, F., "Polymerization in Microemulsions," in *Polymerization in Organized Media*, C. Paleos, ed., Gordon & Breach, Philadelphia, p. 215 (1992).

Candau, F., Y. S. Leong, G. Pouyet, and S. Candau, "Inverse Microemulsion Polymerization of Acrylamide," *J. Coll. Int. Sci.*, **101**, 167 (1984).

Carver, M. T., E. Hirsch, J. C. Wittman, R. M. Fitsch, and F. Candau, "Percolation and Particle Nucleation in Inverse Microemulsion Polymerization," *J. Phys. Chem.*, **93**, 4867 (1989).

Chen, S. J., "Three-Component Cationic Microemulsions: Role of

Curvature in Determining Properties and Structures," PhD Thesis, Univ. of Minnesota, Minneapolis (1985).
Chen, S. J., D. F. Evans, and B. W. Ninham, "Properties and Structure of Three-Component Ionic Microemulsions," *J. Phys. Chem.*, **88**, 1631 (1984).
Chen, S. J., D. F. Evans, B. W. Ninham, D. J. Mitchell, F. D. Blum, and S. Pickup, "Curvature as a Determinant of Microstructure and Microemulsion," *J. Phys. Chem.*, **90**, 842 (1986).
Friberg, S. E., G. Rong, C. C. Yang, and Y. Yang, "Polymerization in Microemulsion," in *Polymer Association Structures*, M. A. El-Nokaly, ed., American Chemical Society, Washington, DC, p. 34 (1989).
Friberg, S. E., A. Ahmed, C. C. Yang, S. Ahuja, and S. Bodesha, "Gelation of a Microemulsion by Silica Formed in situ," *J. Mat. Sci.*, **2**, 257 (1992a).
Friberg, S., C. C. Yang, and J. Sjoblom, "Amphiphilic Association Structures and the Microemulsion/Gel Method for Ceramics," *Langmuir*, **8**, 372 (1992b).
Gan, L. M., C. H. Chew, I. Lye, and T. Imae, "Microemulsion Polymerization of Styrene," *Polym. Bull.*, **25**, 193 (1991).
Glatter, O., and O. Krathy, *Small Angle X-Ray Scattering*, Academic Press, New York (1982).
Gregg, S. J., and K. S. W. Sing, *Adsorption, Surface Area, and Porosity*, Academic Press, London (1982).
Guinier, A., and G. Fournet, *Small-Angle Scattering of X-Rays*, Wiley, New York (1955).
Guo, J. S., M. S. El-Aasser, and J. W. Vanderhoff, "Microemulsion Polymerization of Styrene," *J. Polym. Sci.: Part A: Polym. Chem.*, **27**, 691 (1989).
Guo, J. S., E. D. Sudol, M. S. El-Aasser, and J. W. Vanderhoff, "Particle Nucleation and Monomer Partitioning in Styrene O/W Microemulsion Polymerization," *J. Poly. Sci.: Part A: Polym. Chem.*, **30**, 691 (1992a).
Guo, J. S., E. D. Sudol, M. S. El-Aasser, and J. W. Vanderhoff, "Modeling of Styrene Microemulsion Polymerization," *J. Poly. Sci.: Part A: Poly. Chem.*, **30**, 703 (1992b).
Johnson, P. J., and E. Gulari, "Characteristics of Microemulsion Polymerized Styrene with Water-Soluble versus Oil-Soluble Initiators," *J. Poly. Sci.: Poly. Chem. Ed.*, **22**, 3967 (1984).
Kaler, E. W., "Surfactant Microstructures," PhD Thesis, Univ. of Minnesota, Minneapolis (1982).
Kuo, P. L., N. J. Turro, C. M. Tseng, M. S. El-Aasser, and J. W. Vanderhoff, "Photo Initiated Polymerization of Styrene in Microemulsions," *Macromol.*, **20**, 1216 (1987).
Larpent, C., and T. F. Tadros, "Preparation of Microlatex Dispersions Using Oil-in-Water Microemulsions," *Coll. Poly. Sci.*, **269**, 1171 (1991).
Perez-Luna, V. H., J. Puig, V. Castant, B. Rodriguez, A. Murthy, and E. Kaler, "Styrene Polymerized in Three-Component Cationic Microemulsions," *Langmuir*, **6**, 1040 (1990).
Poehlein, G. W., "Emulsion Polymerization," *Encyclopedia Poly. Sci. Engr.*, Vol. 6, H. Mark, et al., eds., Wiley, New York, p. 1 (1986).
Qutubuddin, S., E. Haque, W. J. Benton, and E. J. Fendler, "Preparation and Characterization of Porous Polymers from Microemulsions," in *Polymer Association Structures*, M. A. El-Nokaly, ed., Amer. Chem. Soc., Washington, DC, p. 64 (1989).
Raj, W. R. P., M. Sasthav, and H. M. Cheung, "Formation of Porous Polymeric Structures by the Polymerization of Single Phase Microemulsions Formulated with Methyl Methacrylate and Acrylic Acid," *Langmuir*, **7**, 2586 (1991).
Raj, W. R. P., M. Sasthav, and H. M. Cheung, "Polymerization of Microstructured Aqueous Systems Formed Using Methyl Methacrylate and Potassium Undecanoate," *Langmuir*, **8**, 1931 (1992).
Raj, W. R. P., M. Sasthav, and H. M. Cheung, "Synthesis of Porous Polymeric Membranes by Polymerization of Microemulsions," *Poly.*, submitted (1994).
Raj, W. R. P., M. Sasthav, and H. M. Cheung, "Microcellular Polymeric Materials from Microemulsions: Control of Microstructure and Morphology," *J. Appl. Poly. Sci.*, submitted (1994).
Walsh, D., J. D. Hopwood, and S. Mann, "Crystal Tectonics," *Science*, **264**, 1576 (1994).

*Manuscript received Oct. 25, 1993, and revision received July 26, 1994.*